



Supplement of

From single storms to large-scale waves: a multi-year kilometer-scale global simulation

Andreas F. Prein et al.

Correspondence to: Andreas F. Prein (aprein@ethz.ch)

The copyright of individual parts of the supplement might differ from the article licence.

TOA LW up, Globe (2020-01-20 to 2024-03-31)

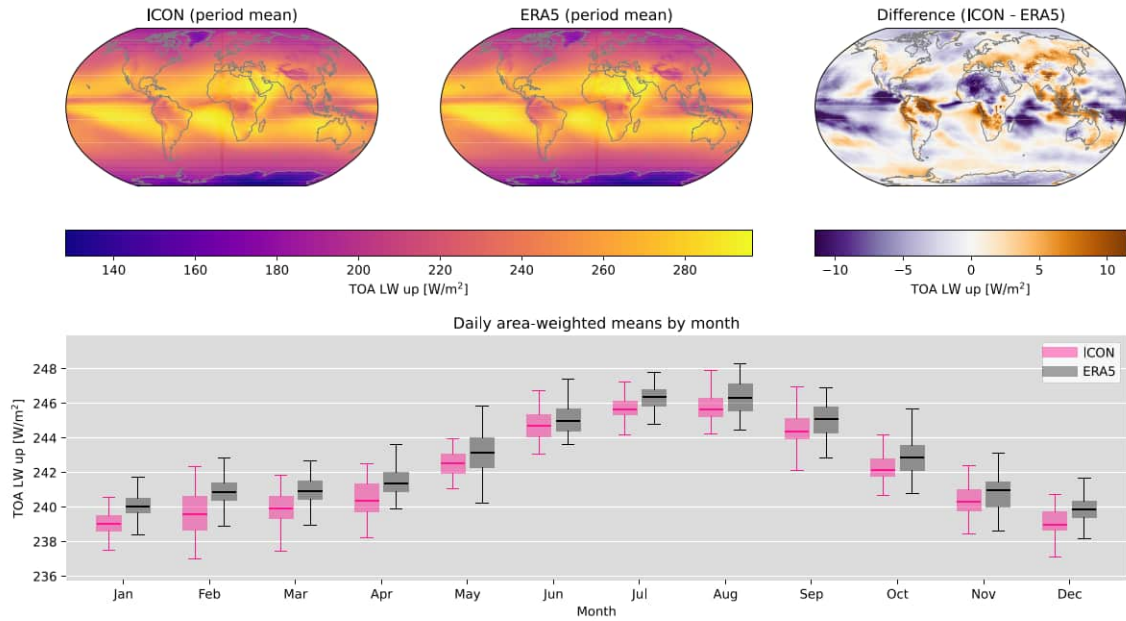


Figure S1. Comparison of top of average atmosphere (TAO) outgoing lowngwave (LW) radiation in ICON (top left), ERA5 (top middle) and their difference (top right). Monthly average global mean statistics are shown in the lower panel.

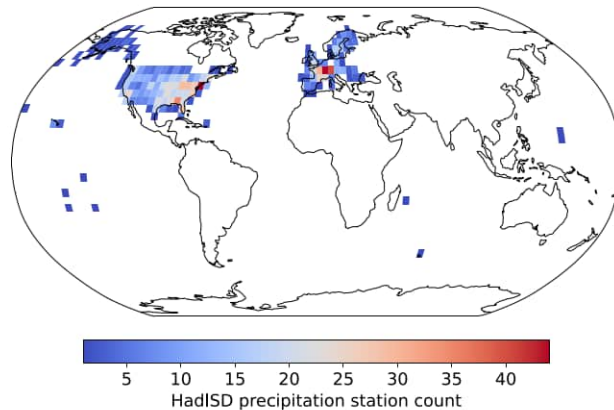


Figure S2. Station density of HadISD precipitation stations that have at least 50 % data coverage during the simulation period in $4 \times 4^\circ$ areas. White areas denote no station coverage.

Precipitation PDFs by IPCC Subregion

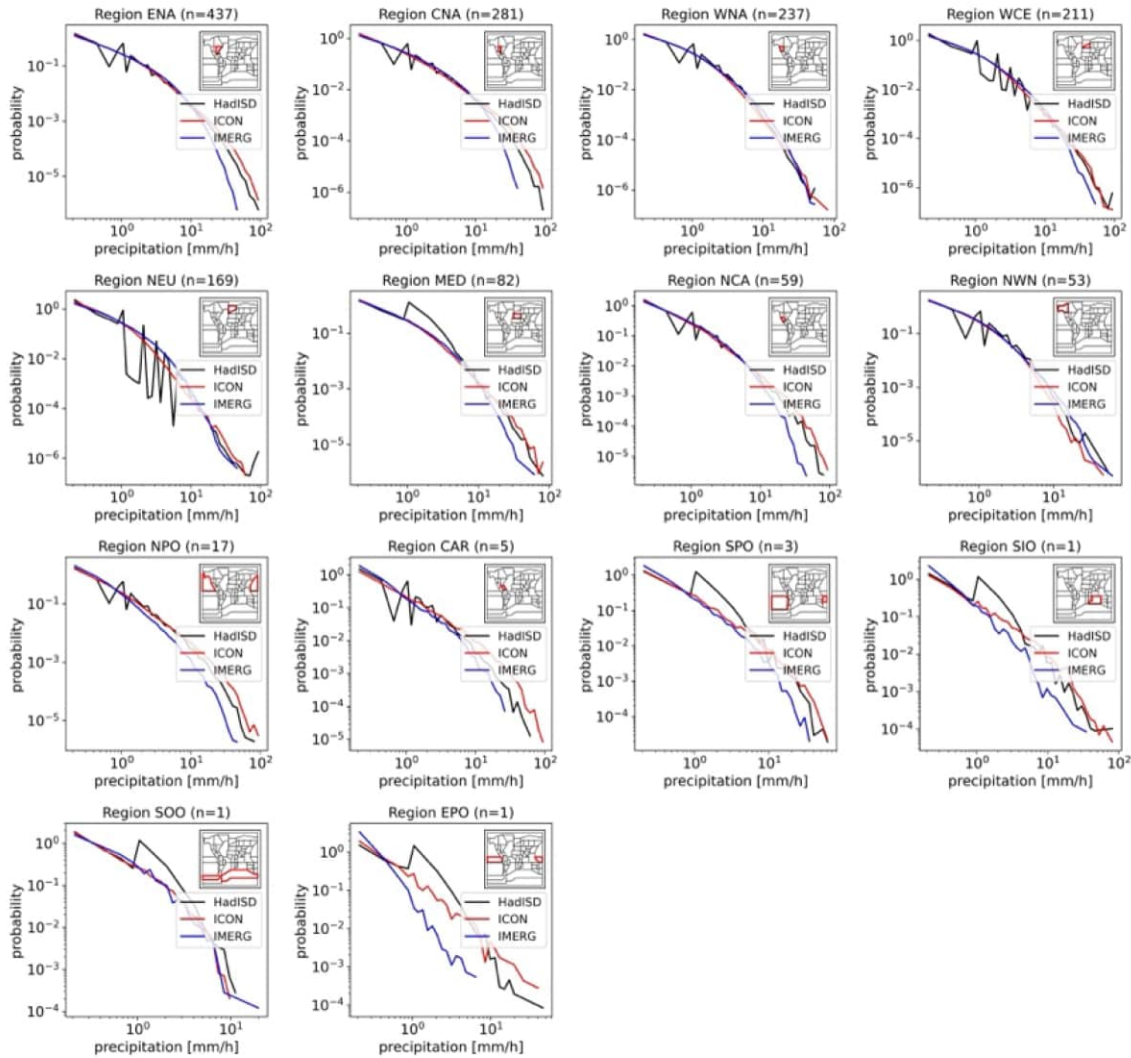


Figure S3. Probability density functions (PDFs) for hourly precipitation comparing ICON (red) and IMERG (blue) against HadISD station observations (black). Shown are Eastern North America (ENA), Central North America (CNA), Western North America (WNA), Western Central Europe (WCE), Northern Europe (NEU), Mediterranean (MED), Northern Central America (NCA), Northwestern North America (NWN), Northern Pacific Ocean (NPO), Caribbean (CAR), South Pacific Ocean (SPO), South Indian Ocean (SIO), Southern Ocean (SOO), and Eastern Pacific Ocean (EPO) from the top left to the bottom right. The locations of these regions are shown in the inlet maps. The underlying station density in the HadISD dataset is shown in Fig. S1 and the number of station (n) in each region is shown in the panel header.

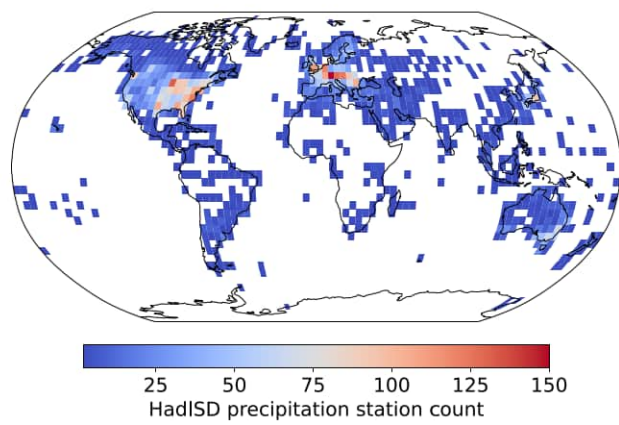


Figure S4. Station density of HadISD 10 m wind stations that have at least 50 % data coverage during the simulation period in $4 \times 4^\circ$ areas. White areas have no station coverage.

Precipitation PDFs by IPCC Subregion

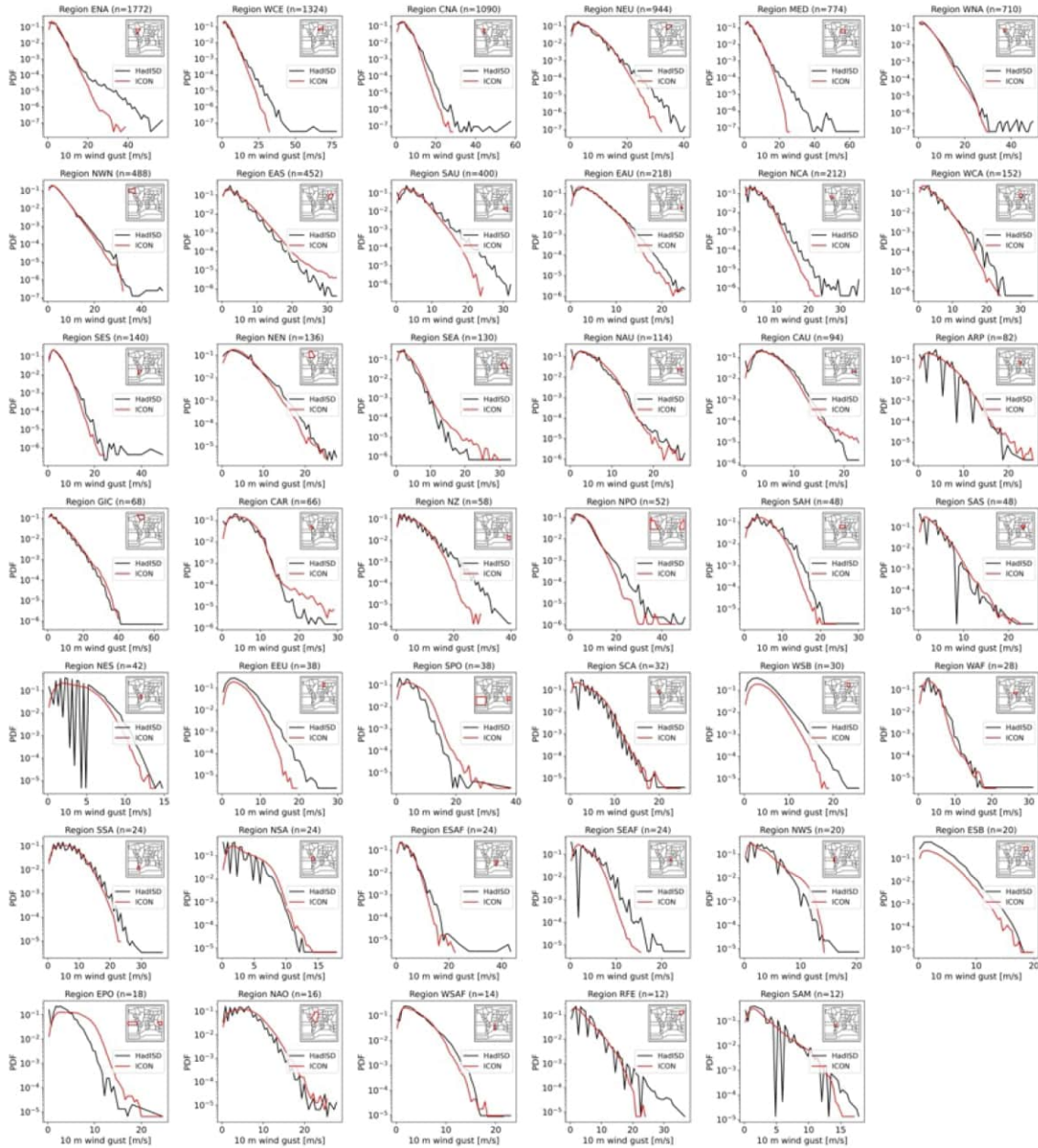


Figure S5. Probability density functions for hourly sampled winds from HadISD (black line) and ICON (red line). Statistics are shown for all stations in various IPCC AR6 regions. The number of stations (n) in each region is shown in the panel titles.

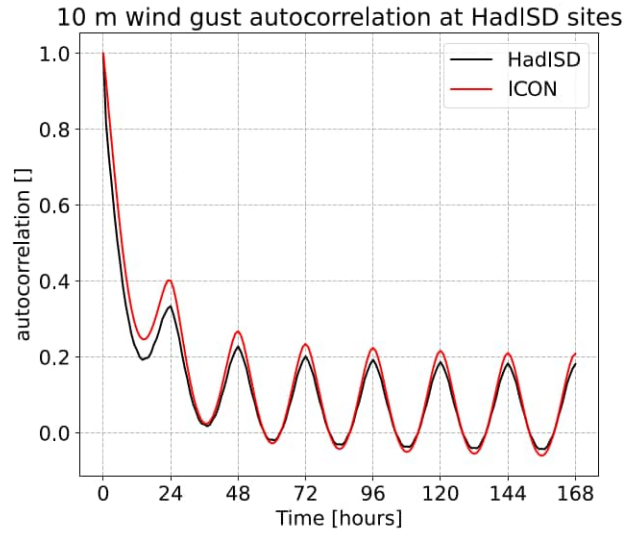


Figure S6. Average autocorrelation of HadISD (black) and ICON (red) 10 m above surface wind gust at the global HadISD sites that have more than 50 % data coverage.

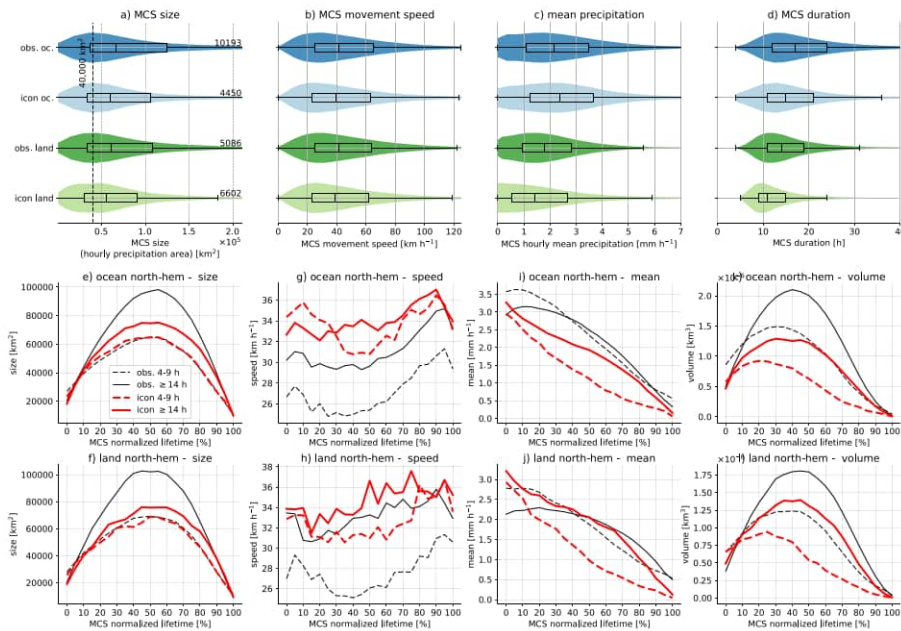


Figure S7. Violin and box-whisker plots for the distribution of northern hemisphere MCS sizes (a), speed (b), mean precipitation (c), and duration (d). The numbers right to the violins in (a) show the number of MCSs in each distribution. The lower panels show the normalized median evolution of short-lived (4-9 hours; dashed) and long-lived (≥ 14 hours; solid) MCSs in GPM observations (black lines) and in ICON (red lines). The middle panels show results for oceans, while the lower panel shows land regions.

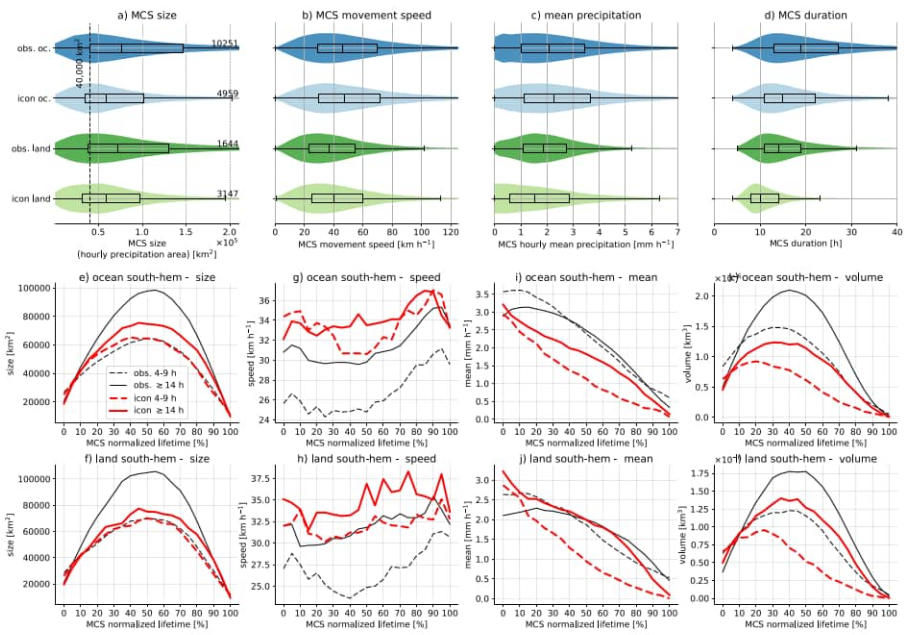


Figure S8. Similar as Fig. S8 but for southern hemispheric MCSs.

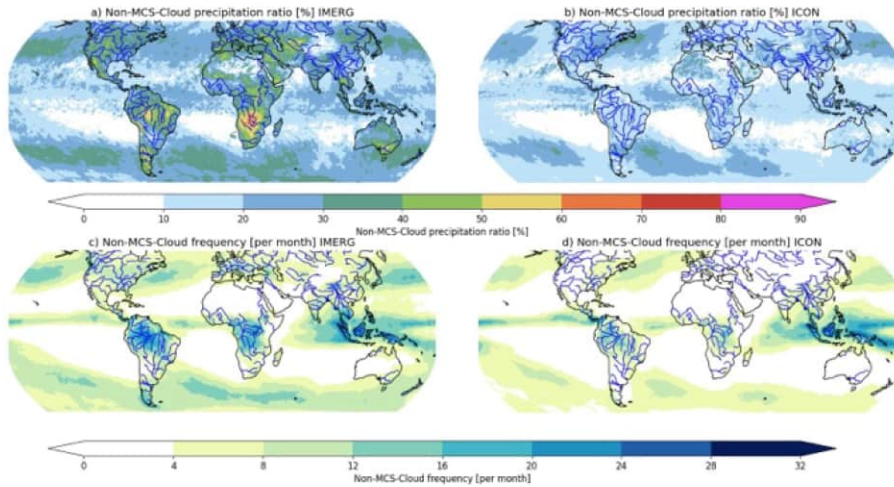


Figure S9. Annual average ratio of non-MCS precipitating cold clouds compared to total precipitation averaged over the simulation period from GPM (a), and ICON (b). The annual average frequency of these clouds in GPM (c), and ICON (d).

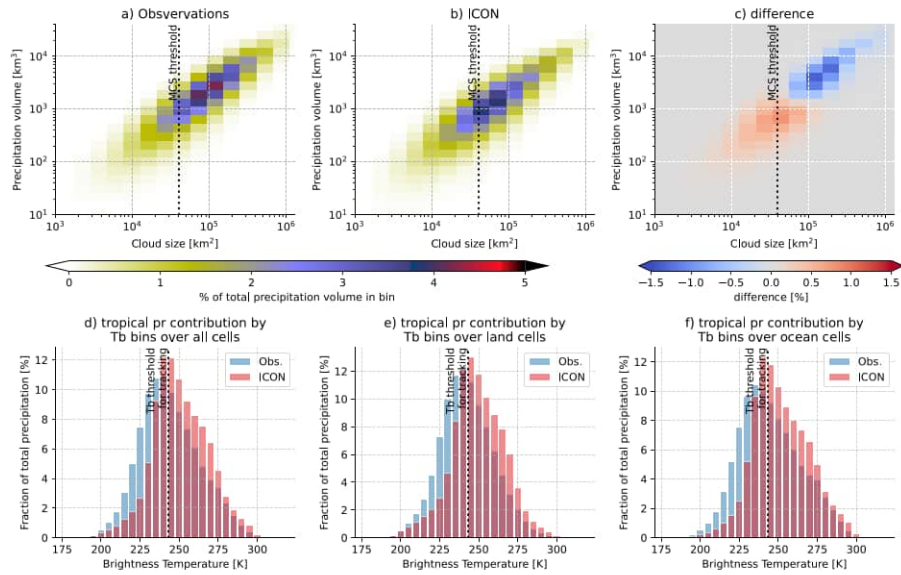


Figure S10. Relative contribution of northern hemisphere (latitude $> 20^\circ < 60$) total precipitation from storms with cold cloud tops ($T_b < 243$ K) as a function of cloud size and precipitation volume under the cloud from observations (a), ICON (b), and their difference (c). The vertical dashed line shows the cloud shield threshold used for MCS classification. The fraction of total precipitation conditioned on T_b over the northern hemisphere (d), northern hemispheric land (e), and northern hemispheric ocean (f). The vertical dashed line shows the T_b threshold used for cold cloud identification.

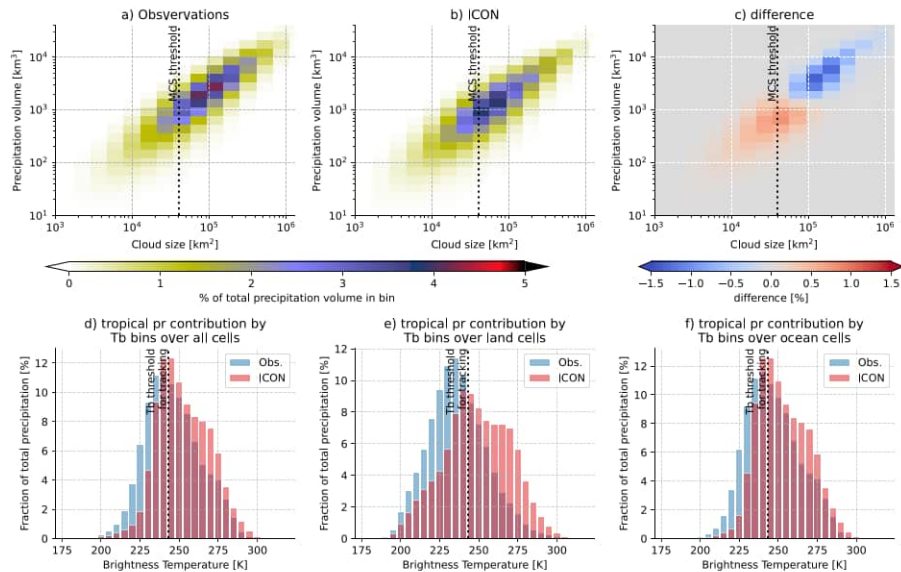


Figure S11. Similar as in Fig. S10 except for the southern hemisphere (latitude $< -20^\circ > -60$).

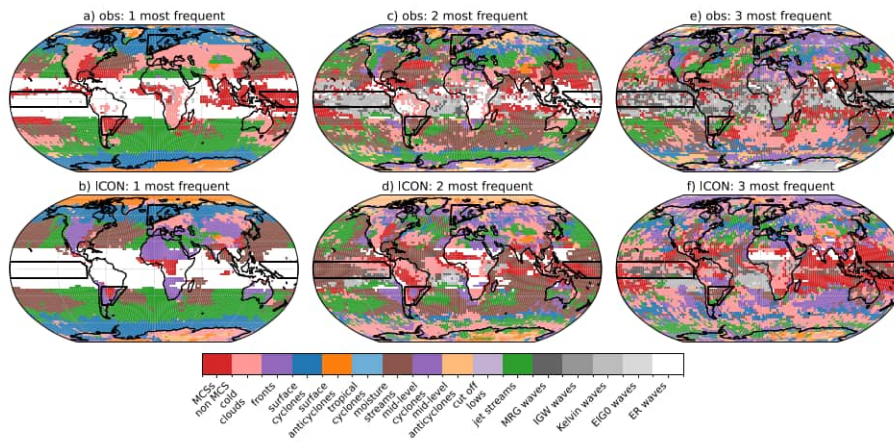


Figure S12. The most frequent (a,b), second most frequent (c,d), and third most frequent (e,f) atmospheric phenomena identified by the MOAAP algorithm that is co-located during the top 20 hourly precipitation events in the evaluation period. Observed/ICON results are shown in the top/middle panel. The data was up-scaled to a 2.5° grid to lower the signal-to-noise ratio.